Mechanical Systems and Signal Processing 25 (2011) 3102–3115

Contents lists available at ScienceDirect

Mechanical Systems and Signal Processing

journal homepage: www.elsevier.com/locate/ymssp

Study of start-up vibration response for oil whirl, oil whip and dry whip

Chen-Chao Fan [a], Jhe-Wei Syu [a], Min-Chun Pan [a,b,*], Wen-Chang Tsao [a]

[a] Department of Mechanical Engineering, National Central University, Taiwan, ROC
[b] Graduate Institute of Biomedical Engineering, National Central University, No. 300, Jhongda Road, Jhongli City, Taoyuan County 32001, Taiwan, ROC

ARTICLE INFO

Article history:
Received 1 September 2010
Received in revised form
28 March 2011
Accepted 19 April 2011
Available online 17 May 2011

Keywords:
Hilbert–Huang Transform
Rub
Whip
Whirl

ABSTRACT

Oil whip induces self-excited vibration in fluid-handling machines and causes self-excited reverse precessional full annular rub, known as "dry whip", which is a secondary phenomenon resulting from a primary cause, that is, "coexistence of oil whip and dry whip". For predicting these instabilities, the clues are hidden in start-up vibration signals of these kinds of machines. This paper presents a method for predicting these kinds of instabilities. First, a Hilbert spectrum combining a full spectrum, which is named the "full Hilbert spectrum", is developed to reveal the whole process. Next, the transient position of a shaft centerline combining an acceptance region is introduced to predict instability at an early stage. The results presented in this study amply demonstrate the transition from stability to instability and the behavior of fluid-induced instability and rub in rotor systems. By this finding, bearing designers can completely understand these instability phenomena existing in fluid-handling machines. As a result, the control parameter for designing controllable bearings can be obtained and the instability problems can be resolved. Consequently, these findings are worth noting.

1. Introduction

Oil whip [1,2] caused by fluid-induced instability is one problem and dry whip induced by rub is another. These kinds of instabilities are serious malfunctions in rotating machinery and may cause a machine catastrophic failure if they occur simultaneously. The oil whip and dry whip involve several major physical phenomena, such as the third bearing effect, friction, impacting, and changes in the system stiffness. The normal operation of machines is affected in such a situation because these instabilities occur repeatedly with constant frequency and amplitude. Moreover, the occurrence of rubbing has two major causes: one is that the oil whip induces instability in a rotating machine and the other is that the desire to increase the efficiency of machines with fluid-film bearings leads to minimize the clearance of seals. However, experiments in this study showed that the coexistence of oil whip and dry whip with almost constant frequency and amplitude occurred in an experimental setup attached with a seal. Though there are some rotor-stator related studies focusing on establishing the symptoms of rotor rub, the transition from stability, oil whirl, oil whip, synchronous precessional full annular rub to the coexistence of oil whip and dry whip were not noticed until recent studies. For observing rub, the full spectrum plot is a good tool but it is insufficient and inappropriate for interpreting nonlinear and non-stationary signals. Therefore, researchers around the world have started using some advanced signal processing techniques, such as the Hilbert–Huang transform (HHT), Wavelets, etc. These tools characterize vibration signals in time–frequency energy representations. HHT developed by Huang and Shen [3,4] is a new method and evolved as a powerful tool for analyzing nonlinear and non-stationary signals.

* Corresponding author at: Department of Mechanical Engineering, National Central University, No. 300, Jhongda Road, Jhongli City, Taoyuan County 32001, Taiwan, ROC. Tel.: +886 3 4267312; fax: +886 3 4254501.
E-mail address: pan_minc@cc.ncu.edu.tw (M.-C. Pan).

0888-3270/$ - see front matter © 2011 Elsevier Ltd. All rights reserved.
doi:10.1016/j.ymssp.2011.04.012

Fluid-induced instability [5] was a dynamic phenomenon resulting from interactions of the surrounding fluid of the bearing in a rotor-bearing system. These interactions produced subsynchronous self-excited vibrations of large amplitude that tracked running speed, which could lead to some severe troubles, such as rotor-to-stator rubbing on seals and bearings, impellers, or other rotor system parts. How to cope with fluid-induced instability has been investigated by previous researchers. Rylander et al. [6] theoretically verified that film thickness and shaft radial velocity and friction could vary by 30% by modifying the shape of an elliptical bearing. Santos and Nicoletti [7] adjusted the bearing geometry by an actuator, which improved the dynamic behaviors of a rotating machine, and developed a four-pad tilting-pad journal bearing (TPJB) that applied the closed-loop system frequency response. Deckler et al. [8] developed an active TPJB with a feedback control system to regulate the orbit of a rotating shaft. Cai et al. [9] proposed an active and stable method of a TPJB with adaptive control. Bently and Hatch [10] explored externally pressurized bearings (EPB). These bearings differed from hydrodynamic bearings in that the fluid was injected at a higher pressure through several circumferentially distributed radial ports. Using the EPB, the oil whirl could partly be eliminated.

A full annular rub [5] was a serious problem because of its destructive effects to rotating machine and could occur in seals or in auxiliary bearings [11]. Muszynska [12] discussed the phenomenon of full annular rub with a 2-DOF model and showed measured results of dry whip triggered by a hammer impact and performed a literature survey on this subject. The results presented in her study were that during the full annular rub, the rotor maintained contact with the seal continuously, and the self-excited reverse precessional full annular rub (dry whip) was more severe than the synchronous full annular rub. Lingener [13] and Crandall [14] demonstrated that dry-friction whirl and whip occurred when the ratio of rotor radius to radial clearance reached 2.66. Childs [15] indicated that dry-friction whirl and whip were only likely to occur at a large seal clearance, and that the triggering of contact normally required an outside disturbance. Yu et al. [16] presented the results of experimental and analytical studies on a rotor-seal full annular rub and both the synchronous and the reverse precession rub were investigated.

Black [17] treated the rub phenomenon that occurred when rotation elements contacted stationary elements in a jet engine. Choi [18] demonstrated the super-harmonics and sub-harmonics in partial rub with an experiment. Peng et al. [19] discriminated the occurrence of a partial rub by the Fourier transforms and time–frequency analysis. Yu et al. [20] showed local Hilbert transform and local Hilbert marginal transform based on empirical mode decomposition (EMD) for the fault diagnosis of roller bearings. Gai [21] presented the use of EMD for the start-up vibration signals and found that the first intrinsic mode function (IMF) could plot Bode plot to obtain some characteristics of rotor systems. Qi et al. [22] demonstrated the use of EMD for the fault diagnosis of rub from the steady state response. Patel and Darpe [23] investigated the potential of the Hilbert–Huang transforms over Wavelet transforms. The appearance of the subsynchronous frequencies in the Hilbert–Huang spectrum is suggested for early rub detection.

Recently, the HHT has been applied in observing the behavior of rotating machines. For the interpretation of rub phenomena, most researches focused on vibration responses at a constant rotating speed. It was less noticed to detect fluid-induced instability and rub with start-up or shutdown vibration signals. This study revealed that the HHT was a useful tool to analyze the start-up signals and was effective for interpreting fluid-induced instability. Hilbert spectral analysis (HSA) showed that oil whirl had a frequency component tracking the rotating speed, and that oil whip had a fixed frequency equal to a natural frequency of the rotor system. However, HSA is insufficient for revealing phenomenon of dry whip. In this paper, first, a Hilbert spectrum combining a full spectrum was developed into the full Hilbert spectrum (FHS), which is an effective method to observe the coexistence of oil whip and dry whip. Next, the transient position of a shaft centerline combining an acceptance region, a powerful tool for observing the transition from stable to unstable conditions, and predicting and preventing the instabilities existing in rotating machinery can be used as a control index to control bearings. Consequently, this notion was thoroughly studied in this paper.

2. Experimental setup and plot interpretation

Predicting fluid-induced instability needs an experimental setup and knowledge about plot identification. For example, the experimental setup can offer data to erect plots, an unfiltered timebase plot can provide important messages to the behavior of rotating machinery, an orbit plot is useful for various kinds of frequency analyses, and an average shaft centerline plot is powerful for detecting and confirming the existence of many machine malfunctions, such as rub, fluid-induced instability, bearing wear or erosion, and misalignment. Through these plots, the malfunctions of rotating machines can clearly be identified and explained. A set of experimental setups and a variety of plots are introduced in order to correctly predict and prevent the instabilities existing in rotating machinery.

2.1. Experimental setup

For observing the phenamena of fluid-induced instability and dry whip, a set of experimental setup was constructed as Fig. 1a. First, a shaft with 9.52 mm diameter and 550 mm length was supported by a relative rigid oilite bronze bushing and a cylindrical fluid-film bearing constructed transparent material through which the journal and the oil fluid film could be viewed, and was driven by a 90 W AC induction motor with a variable speed controller. Two mass disks were attached to the shaft in mid-span. A seal made of bronze was mounted on the middle of the shaft. The fluid-film bearing a diametrical clearance of 0.4 mm was supplied with SAE 10 weight oil mixed with a blue dye that allowed visual inspection

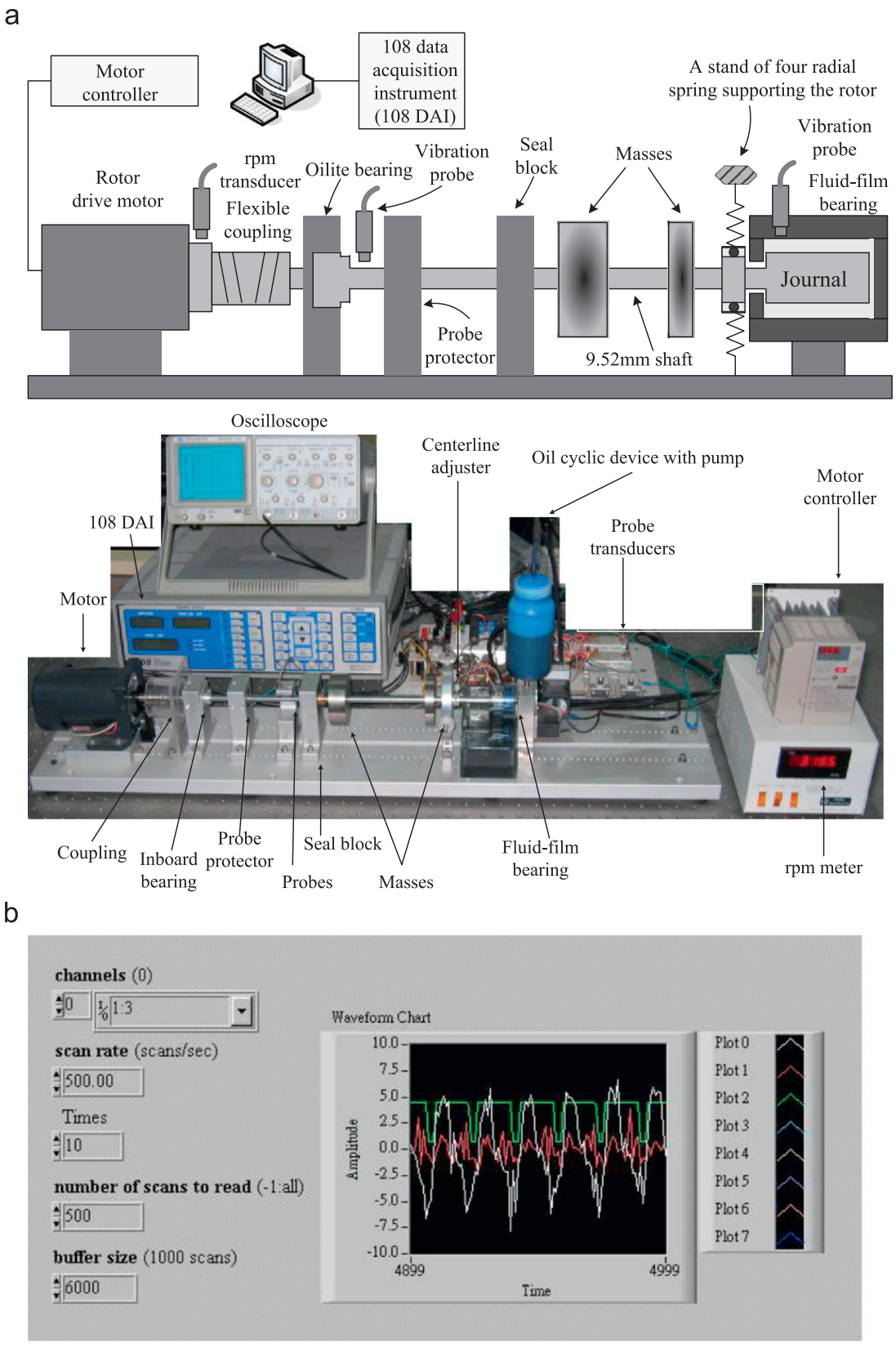

Fig. 1. Experimental setup: (a) schematic diagram and photo of the experimental setup and (b) labview interface.

of the condition of the oil film. The seal with a diametric clearance of 250 μm was used, and the centerline adjuster was carefully adjusted to position the rotor journal to the center of the fluid-film bearing during the experiment. The rotor lateral vibrations were measured by two pairs of eddy current transducers (in *XY* configuration) located at the fluid-lubricated bearing shell and near the seal, respectively, and the photo-sensor (rpm transducer) was installed next to the

flexible coupling in the rotor system to measure the rotor speed. Next, the data capture system included a NI PCI-6024E multifunction card, a 108 data acquisition instrument (108 DAI), and a LabView™ interface (see Fig. 1b). The captured signals were processed by MATLAB® software. Because EMD is severely affected by the shape of the captured signal and the data length, the sampling rate (10 k samples/s) and the sampling time (120 s) must carefully be considered.

2.2. Timebase plot

A timebase plot plays an important role in this paper as it can clearly display the unprocessed output from transducers. If a Keyphasor probe is mounted on rotating machinery, the timebase plot can be used to detect the presence of multiple frequency components. Fig. 2 shows an unfiltered timebase plot with six revolutions of data. First, in the plot, the waveform with the red Keyphasor dots and the black circles are dominated by 1/2*X* vibration, that is, each cycle of vibration has two Keyphasor dots. The Keyphasor dot does not change the position with time, and occurs at another similar relative place in the waveform. This fixed pattern indicates that the vibration frequency is a simple 1/2*X* ratio to running speed. Next, in the same plot (the waveform with the blue Keyphasor dots), the relative vibration frequency is slightly less than 1/2*X*, close to 0.47*X*. For this case, the Keyphasor dot occurs at a slight different vertical place for each cycle of vibration in the waveform. This visual behavior clearly interprets that the relative vibration frequency is not a simple integer relationship to running speed.

The vibration frequency can be examined whether it is slightly less than 1/2*X* or not through the following steps: first, pick a Keyphasor dot as a reference point. Next, move to the right to one complete cycle of vibration (the green line in Fig. 2). While moving to the right, two Keyphasor dots cannot be connected with this green horizontal line. For the complete cycle of vibration, this line should be connected to the green circle. Therefore, the cycle of vibration for two revolutions of the shaft is less than 1/2*X*. In addition, the simplest way to determine the ratio is to observe that the period of vibration is longer than the period for two shaft revolutions; therefore, the frequency of the vibration is less than 1/2*X*. What can be concluded from these interpretations? If the frequency of the vibration is exactly 1/2*X* component, the Keyphasor dots do not change their positions. Conversely, if the frequency of the vibration is less than 1/2*X* component, the Keyphasor dots change their vertical positions.

2.3. Orbit plot

Rotation is the angular motion of the rotor about its shaft centerline. Precession is the lateral motion, or vibration, of the rotor geometric center in the *XY* plane, which is perpendicular to the axis of the rotor. Precession is also known as orbiting or vibration; the orbit is a display of the lateral motion of the shaft centerline. Precession is completely independent of rotation. It is possible for a rotor to rotate without vibrating. Conversely, it is possible for a rotor to vibrate without rotating. Usually, however, both rotation and precession occur at the same time.

An orbit represents the path of the shaft centerline relative to a pair of orthogonal eddy current transducers. These transducers are usually mounted rigidly on the machine casing near a bearing; thus, the orbit typically represents the path of the shaft centerline relative to the bearing clearance of the machine. Because of its ease of interpretation and extensive information content, the orbit, with Keyphasor marks, is probably the most powerful single plot format available to the machinery diagnostician. Also, the precession direction of a rotating machine can be determined by a blank/dot sequence (offered by a Keyphasor probe) on the orbit plot (see Fig. 3).

Fig. 3 shows an orbiting rotor (the size of the orbit is greatly exaggerated) that is viewed by two orthogonal transducers. As the rotor rotates, the shaft centerline also moves (precesses) along a path that defines the orbit. A Keyphasor probe is installed to detect a once-per-turn mark on the shaft, in this case a notch. When the leading edge of the notch passes next to the Keyphasor probe, the transient position of the shaft centerline is located at the Keyphasor dot on the orbit (position 3 in Fig. 3). The Keyphasor signal is like a strobe that briefly illuminates the shaft as it travels in its orbit. Even though the

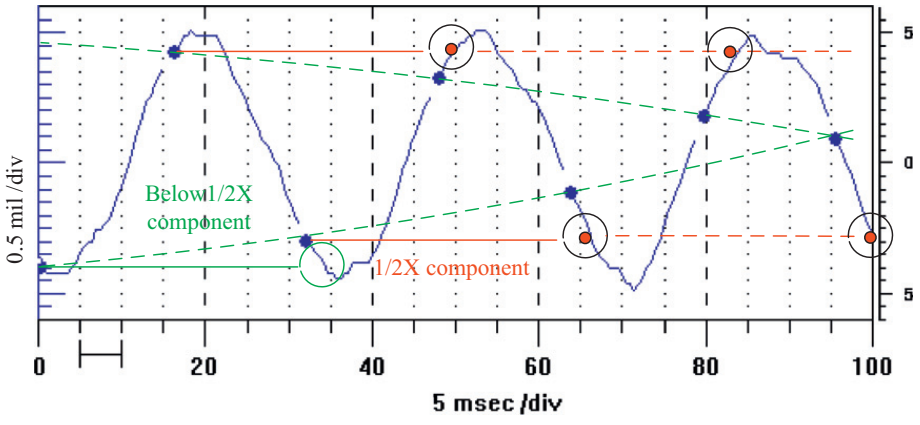

Fig. 2. Timebase plot that interprets the difference between exact 1/2*X* and Not-1/2*X*. (For interpretation of the references to color in this figure, the reader is referred to the web version of this article.)

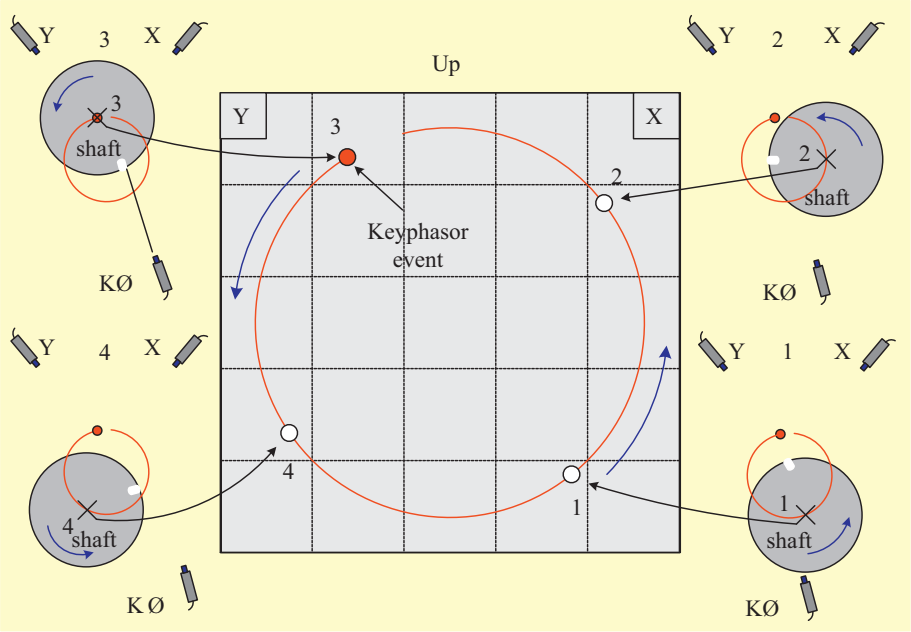

Fig. 3. Orbit plot. The Keyphasor probe detects the notch at position 3. At the moment, the shaft centerline is located at the position of the Keyphasor dot on the orbit plot.

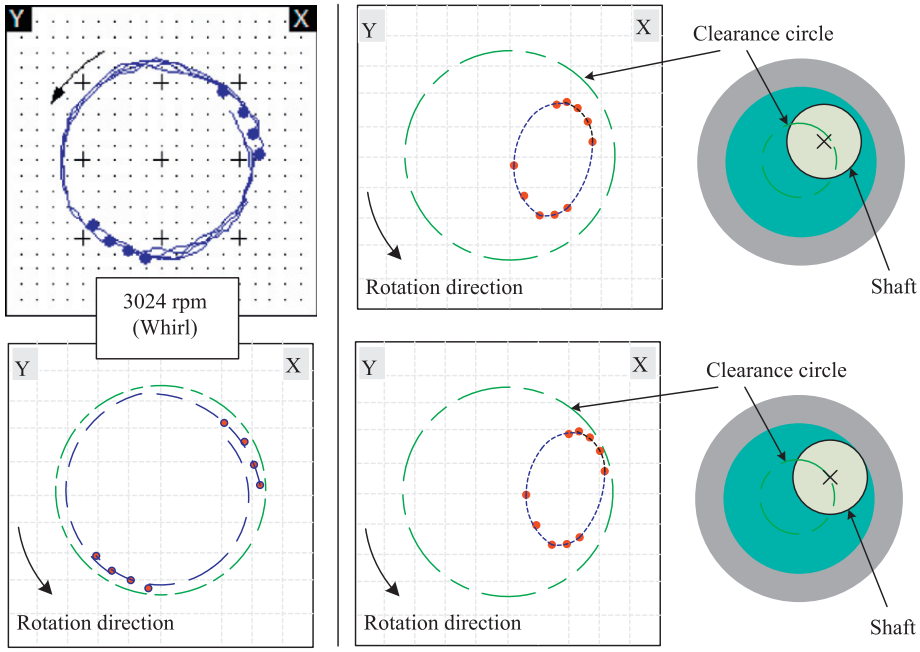

Fig. 4. Average shaft centerline plot. At the middle, the red dot (each cycle of vibration has one or two dots, depending on 1*X* or 1/2*X*) represents the transient position of the shaft centerline when the Keyphasor event occurs. The consecutive dots can form an orbit that is the path traced out by the transient positions of the shaft centerlines as the shaft walks around the bearing with increasing speed. (For interpretation of the references to color in this figure legend, the reader is referred to the web version of this article.)

rotor is on the opposite side of the orbit from the Keyphasor probe, the notch on the shaft is in a position to be sensed by the Keyphasor probe (see position 3 in Fig. 3).

2.4. *Average shaft centerline and acceptance region plot*

Fig. 4 shows the dynamic motion of the shaft centerline about an average position that is constructed from the ac part of the vibration signals. In this paper, the average shaft centerline plot changes with the average positions of the shaft centerlines in two dimensions and is constructed from the consecutive, dynamic motion of the shaft centerlines about an average position, that is, the red dots (each cycle of vibration has one or two dots, depending on 1*X* or 1/2*X*) represent the position of the shaft centerline when the Keyphasor event occurs. The consecutive dots can form an orbit that is the path

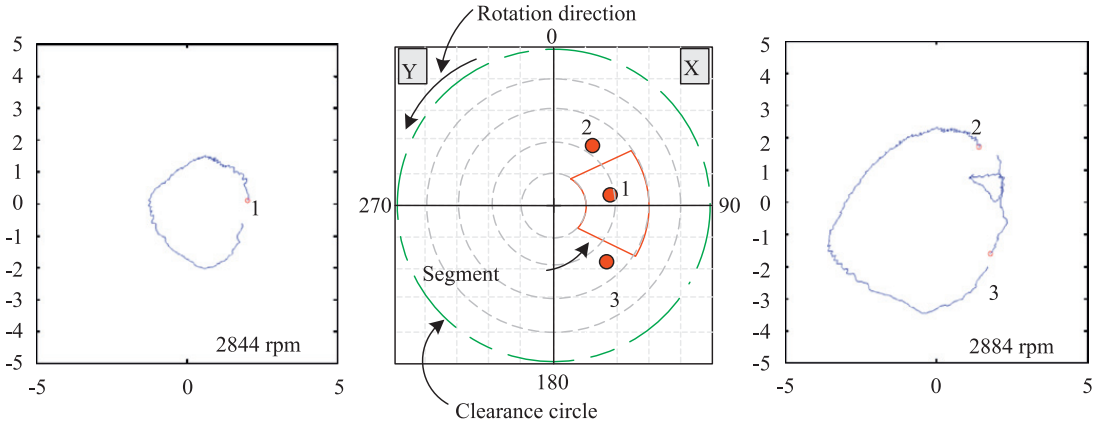

Fig. 5. Acceptance region plot with the segment (sector), which can be defined with various boundaries. The segment can be arbitrarily set according to the running conditions of a rotor system.

traced out by the transient positions of the shaft centerlines as the shaft walks around the bearing with rotor speed. When a set of such data is collected versus speed, the plot becomes an average shaft centerline plot. In addition, in a machine with internally pressured (hydrodynamic) fluid-film bearing, the changes in rotor speeds will usually produce a change in average shaft positions. This happens because the stiffness of the bearing changes with rotor speed, namely, the stiffness is a function of speed. This is the reason why fluid-induced instability occurs.

Fig. 5 shows an acceptance region plot [24]. The boundary extremes and the position of the segment (or sector) in Fig. 5 will differ for various machines, and hence a prior knowledge of likely or acceptable variations will be useful. The region within the boundaries of a segment is termed as the acceptance region, which is useful for detecting and confirming the existence of many machine malfunctions, such as rub, fluid-induced instability, bearing wear or erosion, and misalignment. In the middle plot, mark 1 (the shaft centerline position) inside the segment, for example, is an allowable operating range. If the shaft centerline positions are outside the segment (marks 2 and 3 in Fig. 5), it means that the machine has some malfunctions. Because these malfunctions can produce noticeable changes in the behavior of shaft centerlines, the transient position of a shaft centerline combining with an acceptance region, segment, and clearance circle (it is equal to the bearing diameter minus the shaft journal diameter, the diametric clearance) is a very important tool when performing diagnosis. This segment is most important because it can arbitrarily be set according to the running conditions of a rotor system. Some malfunctions can happen if the transient positions of the shaft centerlines of a rotor system deviate outside the segment. By this technique, most controllable bearings can apply the acceptance region as a control parameter to predict and prevent instability.

2.5. Partial and full annular rub

Rub [5] is an undesired contact between a rotating and a stationary part and it is always a secondary effect that is caused by fluid-induced instability that uses up the available clearance between the rotor and the stator. It can be categorized as follows: when a contact occurs over a small fraction of the vibration cycle, it is called the partial rub. When it occurs over the entire vibration cycle, it is called the full annular rub.

What is the difference between fluid-induced instability and rub? The fluid-induced instability produces subsynchronous vibration that is sometimes misdiagnosed as a rub. Generally, there are two aspects of subsynchronous vibration that help discriminate between the malfunctions. First, subsynchronous vibration due to rub will usually lock to a simple integer ratio frequency (1/2*X*, 1/3*X*, etc.) while fluid-induced instability is most likely to produce vibration at a non-integer ratio (such as 0.47*X*). Second, the full spectrum can clearly show that rub will tend to have a significant reverse component but fluid-induced instability tends to be predominantly forward [5]. Also, the subsynchronous component of the rub orbit is extremely elliptical and that of the fluid-induced instability orbit is forward and nearly circular. In the rub orbit, the Keyphasor dots are locked, indicating exact 1/2*X* vibration; in fluid-induced instability orbit, the Keyphasor dots move around the orbit forward path.

The diagnosis is rather complicated because the subsynchronous vibration with large amplitude due to fluid-induced instability can create a rub. Both rub and fluid-induced instability may be active at the same time. They have a similar rotor dynamic property, that is, the subsynchronous vibration is associated with a natural frequency of the rotor system. Generally, the direct orbit with Keyphasor dots and the full spectrum are the best tools for discriminating them.

2.6. Hilbert–Huang transform and full spectrum plot

2.6.1. Hilbert–Huang transform

The Hilbert–Huang transform was brought out by Huang in 1998 ([4] including the references therein). The process is briefly described as follows: the HHT includes two procedures, namely, the EMD and the Hilbert spectrum analysis (HSA).

First, the EMD decomposes multi-component signals into a number of intrinsic mode functions (IMFs). Each IMF represents a mono-component function with respect to time. Next, the Hilbert transform (HT) and the analytic signal concept are applied to compute the instantaneous amplitude and frequency of each IMF. Finally, the Hilbert spectrum can show the time–frequency distribution and interpret physical meanings embedded in IMF.

In general, any IMF must satisfy two conditions: (a) the number of extrema and the number of zero crossings must be either equal or different at most by one in a whole data set; (b) at any point, the mean value of two envelopes defined by the local maxima and the local minima is zero. The decomposition procedure of the EMD is called the sifting process (SP).

2.6.2. Full spectrum plot

The full spectrum [25,26], which was developed using an orthogonal pair of vibration transducers, reveals additional information and can be used to analyze transient and steady signals, which a half spectrum cannot provide. Generally, half spectrum of a single vibration signal is used to identify frequency components for diagnosing machinery malfunctions. Unfortunately, the hidden information regarding the correlation between the two vibration signals may be ignored. The full spectrum plot characterizes the relationship between the orbit constructed from the *X*- and the *Y*-direction vibration signals and the direction of rotor rotation, and determines whether the rotor orbit or the shaft motion is forward or reverse, which is relative to the direction of rotor rotation.

For obtaining a full spectrum, some basic concepts must be understood. First, two timebase signals are filtered at a certain frequency and can form a filtered orbit. Next, a filtered orbit with an elliptical shape is a combination of two circular orbits, that is, one is a locus of the vector rotating in the direction of rotation (forward) and the other is a locus of the vector rotating in the opposite direction (reverse). Finally, the length of the forward vector is the amplitude of the positive frequency and the length of the reverse vector is the amplitude of the negative frequency.

For demonstrating the advantages of a full spectrum, the signals from a pair of vibration transducers located at the fluid-film bearing of the rotor system while running from 6306 to 6307 rpm were processed using the full spectrum as an example. As shown in Fig. 6, the unfiltered data has many frequency components, such as revolution and precession speed, and the unfiltered orbit is too disordered to indicate any information for malfunction diagnosis. The two signals are filtered by a band-pass filter set at 0.47*X* (49 Hz) and 1*X* (105 Hz). The filtered orbit is a pure ellipse. The pure ellipse (blue line) is a sum of two circles (in red and black color). As the machine is rotated counterclockwise, the blue vector, which presented the path of the filtered orbit, is rotated in the same direction with the machine. The red vector moved counterclockwise (forward), but the black vector moved in the opposite direction (reverse). Both the vectors rotate at the same frequency (the frequency of the filtered orbit). The length of the red vector is the amplitude of the positive frequency and the length of the black vector is the amplitude of the negative frequency.

2.7. Full Hilbert spectrum

The purpose of data processing is to extract and display the main components of the information from raw data generated by transducers. The full Hilbert spectrum (FHS) allows one to determine whether fluid-induced instability and dry whip are forward or reverse in relation to the direction of rotor rotation. This information, which is characteristic of specific machinery malfunctions, makes the FHS become a powerful tool for interpreting instability existing in rotating machinery.

Fig. 7 shows the flowchart of the algorithm of the FHS, which is based on the full spectrum and the Hilbert transform (see Section 2.6). The process of creating the FHS is described as follows:

Step 1. Obtain raw data from transducers of rotating machinery and separate the data into some small period signals through its resonance. After being filterred and combined, these signals generate orbits, namely, pure ellipses.
Step 2. Find the major and the minor axis of the ellipses and compute two diameters of forward and reverse rotational circle. The diameters are the frequency components. After the above steps are performed, the information obtained is enough to show the phenomena of rotating machinery.
Step 3. Reconstruct these frequency domain signals into the time domain signals.
Step 4. Applying the analytic signal computation, the FHS can be obtained. The forward and reverse signals are transformed seperately, and are combined to obtain the FHS. In the FHS, the spectrum of forward precession frequencies is on the horizontal positive axis and the spectrum of reverse precession frequencies is on the negative horizontal axis.

Now one knows how an FHS is created, and what important information it contains. In order to perform reliable diagnostics, all possible informations have to be extracted from the original data. Since the FHS contains more information than others, such as the half spectrum, it has an advantage from that perspective. It can be used for steady state and transient analysis.

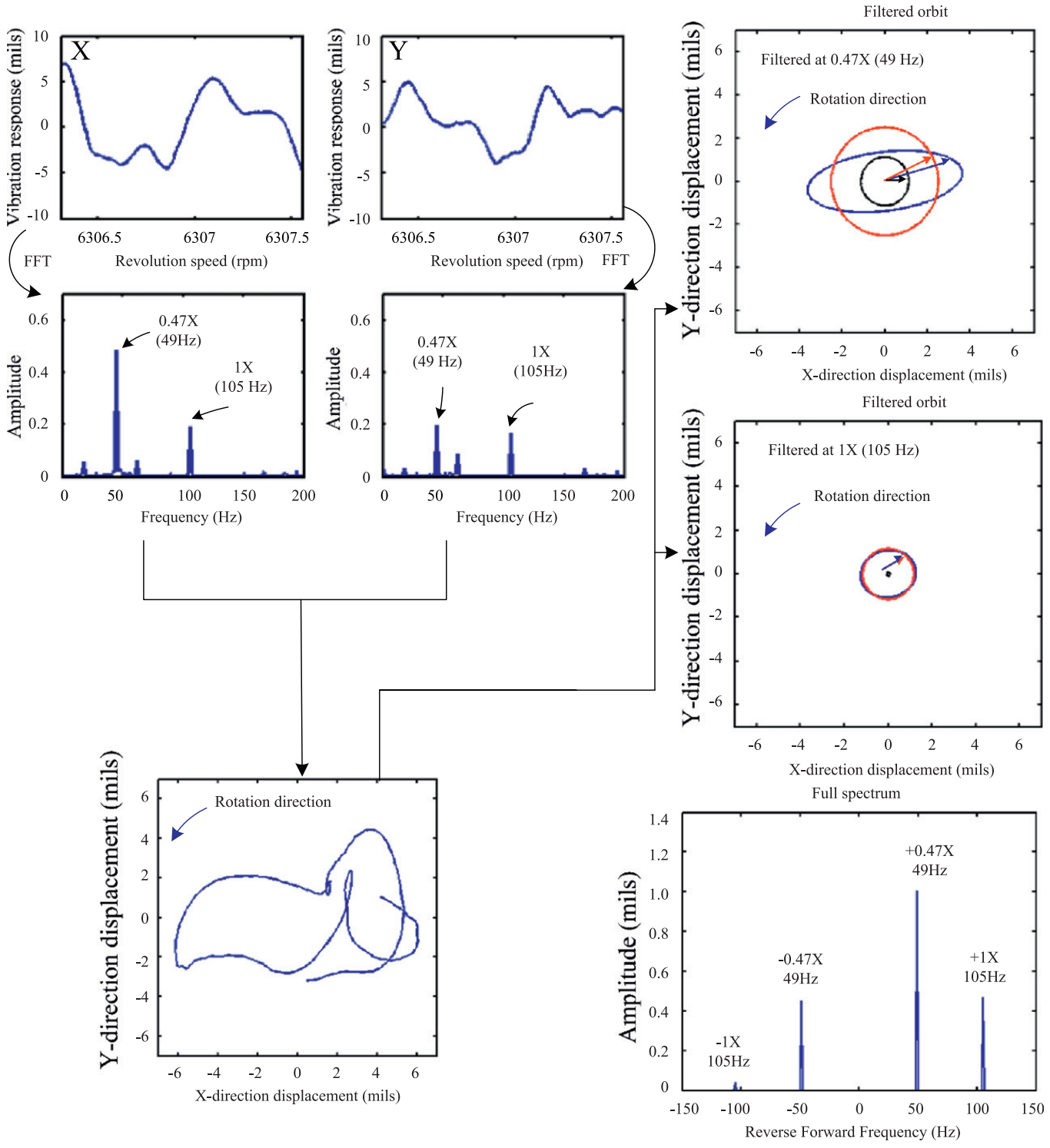

Fig. 6. Example of the full spectrum plot.

2.8. *Differences between full spectrum and full Hilbert spectrum*

There are different advantages of the full spectrum (FS) and the full Hilbert spectrum (FHS). Combining each other, the fault phenomena existing in rotating machinery can more easily be distinguished and addressed. The fault of fluid-induced instability and the dry whip are the same kind of signals in rotor systems, namely, both are non-stationary and self-excited vibration signals. Therefore, the FS cannot meet the requirement of non-stationary time varying signals and time–frequency analysis. The FHS method was applied to the detection and the time–frequency analysis of fluid-induced instability and dry whip. From the FHS, the dimidiate frequency of fluid-induced instability and dry whip was definitely found. This clearly reveals the properties of fluid-induced instability and dry whip, and provides information for early fault

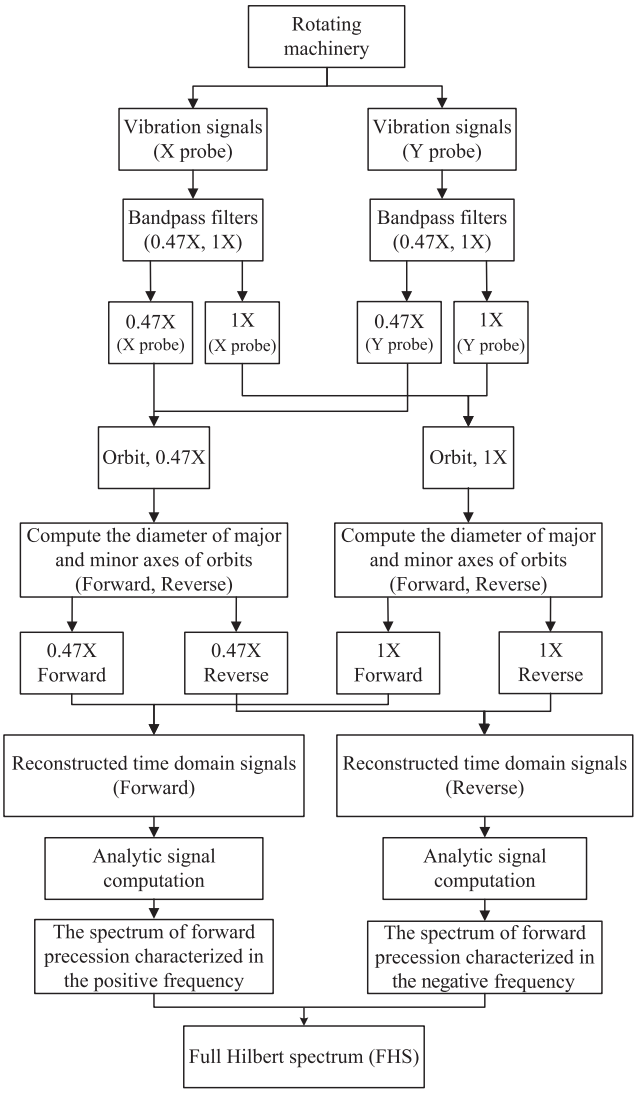

Fig. 7. Flowchart of FHS.

diagnosis. With the proposed method, development of the coexistence of oil whip and dry whip was displayed and the time, frequency, and amplitude information can be accurately detected, which provided time information for this kind of fault diagnosis. Inversely, due to resolution, the FS cannot clearly reveal the occurrence of time. However, both the FHS and the FS are powerful tools when carefully applied. Because of its wide availability, there is temptation to use the spectrum plot to the exclusion of other plot formats. But the spectrum, however, powerful, is not a substitute for the information that can only be obtained in other plots: the filtered amplitude and phase in polar and Bode plots, the shaft position information in average shaft centerline plots, the shape and frequency information in the orbit, and the waveform information in the timebase plot. All these informations are needed for comprehensive machinery management.

Rotating machinery monitoring and diagnostics are gradually evolving. However, even from what ones know now, this new data presentation format, namely, FHS, is worth using. It provides the energy spectrum to observe fluid-induced instability and rub, and gives a better foundation for root cause analysis. The energy spectrum makes the engineers working in power plants more easily notice the fault phenomena existing in rotating machinery, compared to the FS, which shows only the frequency components and amplitude of vibration signals.

3. Experimental study

3.1. Observed vibrational phenomena using HHT

The HHT is an excellent tool for observing and interpreting a nonlinear phenomenon like fluid-induced instability. Recently, the most significant aspect of studies is to identify the onset of instability from start-up vibration signals. In the experiment here, a seal signal was decomposed into 18 IMFs. It is noted that the EMD processing is a band-pass filtering procedure to shift signal components from a higher spectral band to a lower spectral one. In the upper part of Fig. 8, the

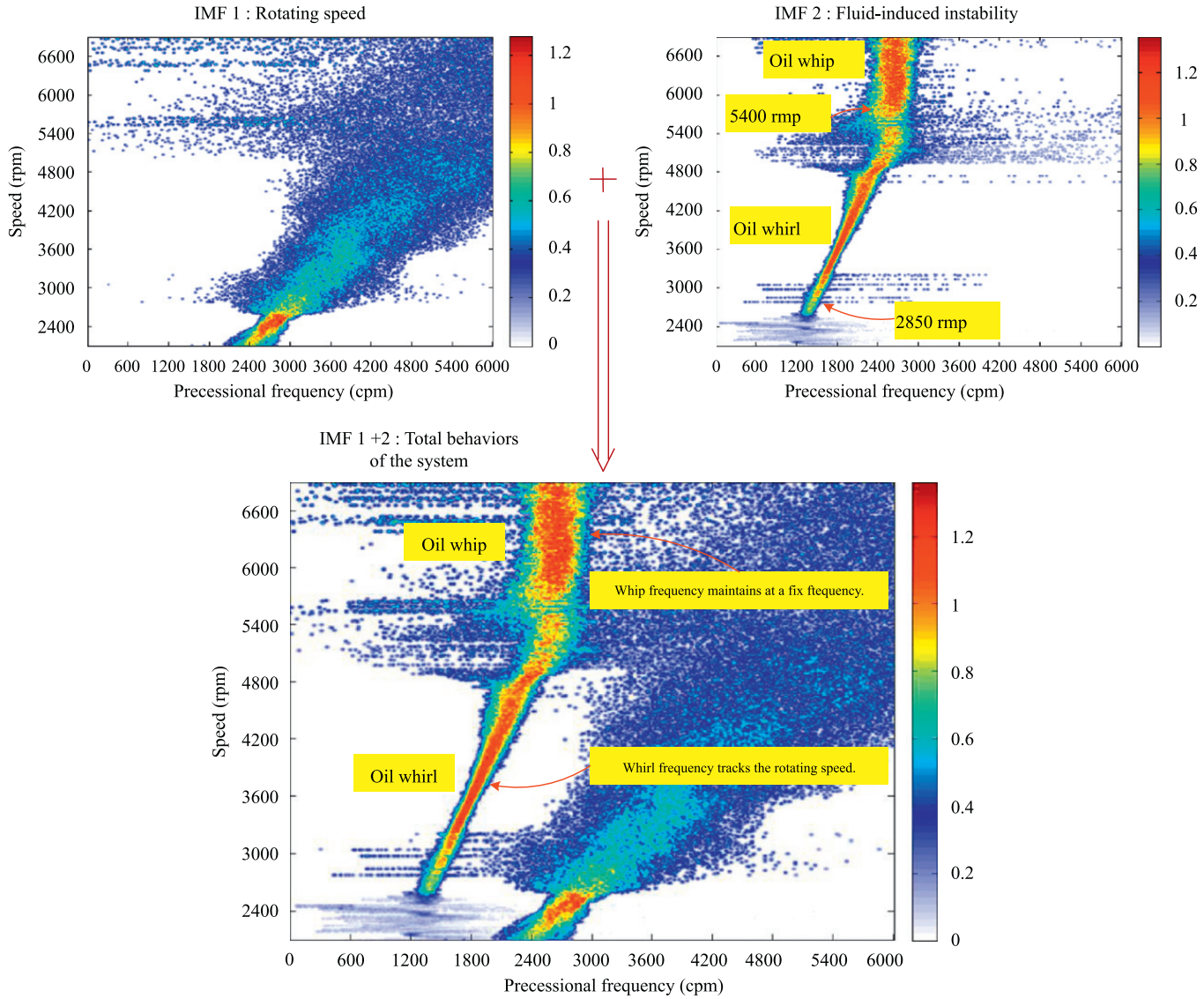

Fig. 8. Hilbert spectrum plot. Vibration signal is obtained from the horizontal direction of the seal.

Hilbert spectrum of IMF 1 characterizes the phenomena of the rotor speed (1*X*) above 2400 rpm, and the spectral component characterizing oil whirl and whip is extracted through IMF2. For other IMFs showing even lower-frequency signatures, no significant events can be set apart.

The whole behavior of the rotor system can be revealed by combining IMF1 and IMF2, the lower part of Fig. 8. The oil whirl occurred at about 2850 rpm, and the rotor is rotated with subsynchronous frequency tracking the rotating speed. The Hilbert spectrum also showed the energy distribution changing from the stable to unstable conditions. When the rotating speed was increased to 5400 rpm, the rotor system entered the whip stage and rotated with an almost fixed frequency. The HHT provides a clear message about that the IMF2 definitely reveals the oil whirl and whip phenomena but cannot show any information about rub because it occurs in reverse spectrum. Consequently, in this paper, the full Hilbert spectrum is developed to observe the coexistence of oil whip and dry whip, and is discussed in detail in the following section.

3.2. *Observed vibrational phenomena using full Hilbert spectrum*

In this section, the FHS is used to obtain more information. Generally, the analyzed method like the Fourier transform cannot provide the information of negative frequencies, but it is important for diagnosing some malfunctions of rotating machinery like rub, which usually produces reverse components on the full spectrum and can generate high vibration and rapidly destroy machines.

Fig. 9 shows the FHS at the fluid-film bearing and seal. The spectrum of forward precession frequencies is on the positive horizontal axis and the spectrum of reverse precession frequencies is on the negative horizontal axis. The rotor speed is on the vertical axis. The color means the vibration amplitude of the corresponding frequency. The redder the color,

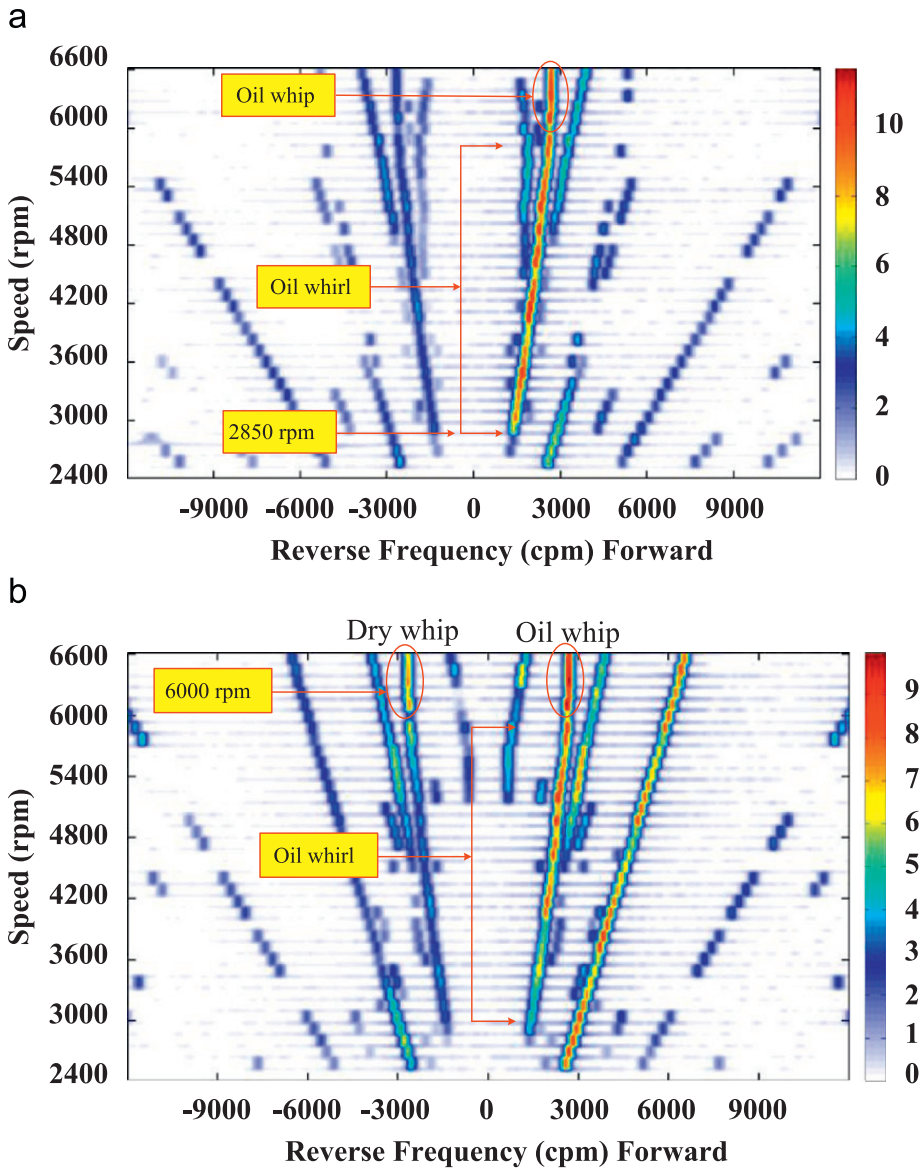

Fig. 9. Full Hilbert spectrum plot: (a) vibration signal measured from the fluid-film bearing and (b) vibration signal measured from the seal.

the bigger the vibration. The FHS can describe the whole behavior of the rotor system, such as oil whirl, oil whip, and rub, in a color plot. Fig. 9a and b shows the FHS of the instability phenomena at the fluid-film bearing and at the seal, separately. The whirl instability occurred at about 2850 rpm. In this period, the shaft of the rotor contacted the stator lightly. The FHS at the fluid-film bearing did not clearly indicate the partial rub phenomenon because the probe was far from the seal and the reverse precession vibration was too small to be shown on the FHS.

The FHS at the seal provides a good view of rub phenomenon. With the increasing rotor speed, the rub became severe. In the whirl stage, the vibration amplitude at the seal was too small to be clearly shown on the FHS. When the rotor speed reached 6000 rpm, the system entered the whip stage. The behavior of the rotor system was the first bending mode, and the vibration was bigger so that the shaft contacted the stator and the rub became more severe. Fig. 9b clearly shows the coexistence of oil whip and dry whip, which cannot be shown on the HS. This is the reason why the FHS is developed.

One thing to note is that the property of self-excited reverse precessional full annular rub, known as "dry whip", [16] is the same as oil whip, but it belongs to reverse precessional behavior while the oil whip belongs to forward precessional behavior. They both run with an almost constant frequency and amplitude, and occur in forward (oil whip) and reverse (dry whip) directions of the full Hilbert Spectrum plots, separately. Therefore, both components can be shown in the FHS of Fig. 9b.

4. Cause and effect analyses

The transition from stable to unstable conditions is an important clue for predicting and preventing fluid-induced instability. In this paper, the timebase and the orbit plot are well studied in order to interpret the transition. Fig. 10 shows

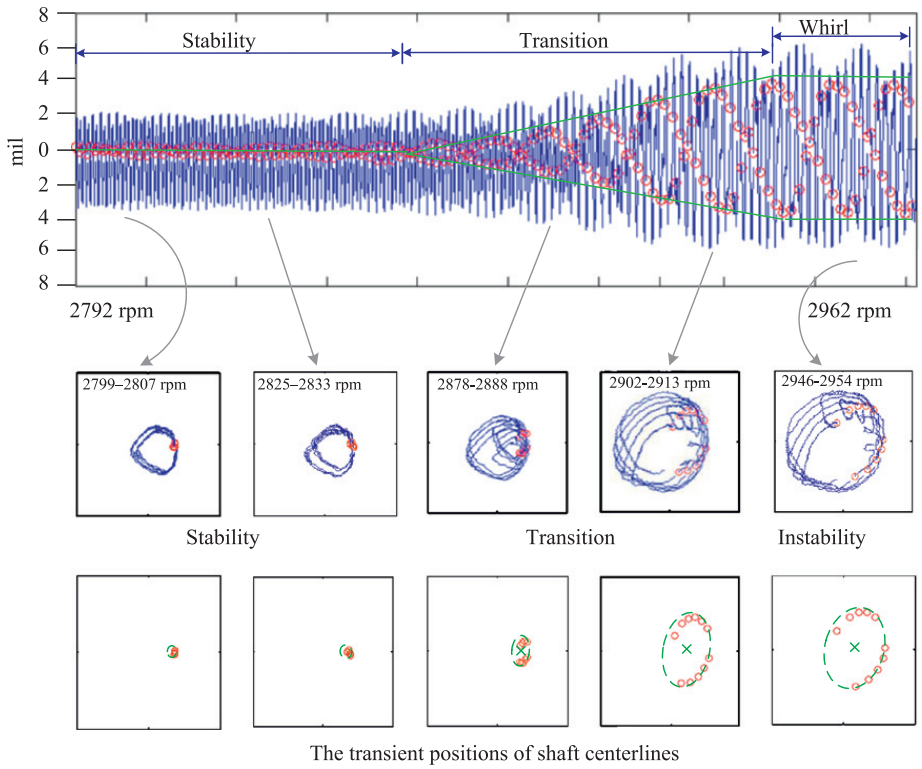

Fig. 10. At the top, the timebase plot reveals the transition from stability to whirl. At the middle, the orbits with the Keyphasor marks exhibit the changes in the transient positions of the shaft centerlines. At the bottom, the orbit plot shows the transition from 2792 to 2962 rpm.

the transition of the transient positions of shaft centerlines. The raw data was obtained from the *X*- and *Y*-probe located at the fluid-film bearing of the rotor system while operating during the start-up. At the top, the timebase plot exhibits that the signals experience a process from stability, transition from stability to instability, to oil whirl. In the stable region, the vibration amplitude was fixed while the rotor speed was 2805–2854 rpm. The rotor system was running steadily and its phase did not almost change. With the increasing rotor speed, the rotor system entered the unstable region. In this region, the amplitude and the phase of the vibration were growing and changing rapidly. When the rotor system entered the whirl region, the amplitude of the vibration was almost constant but the phase was changing rapidly. At the middle, there are five orbit plots and each of them includes several orbits. This clearly shows the transitional process from stability to instability. First, the size of the orbit was kept constant when the rotor system was operated at the stable region. With the increasing rotor speed, the rotor system began to enter an unstable region. It was not the whirl region. It was called transition because it fluctuated between the stable and the whirl region. In this transitional region, the amplitude and the phase of the orbit to be observed were growing and changing fast. The changes in this period provide important messages to bearing designers who design the control system because it clearly offers a clue as a control index, that is, the transient positions of the shaft centerlines were changing fast with rotor speed. The rotor speeds from 2862 to 2922 rpm are the transitional region because this period from stability to instability in a rotor system is normally experienced in this process. At the bottom, the orbit plots exhibit the changes in the transient positions of the shaft centerlines (or the Keyphasor dots) while the rotor system was operating at a speed of 2792–2962 rpm. The transient position of the shaft centerline representing the phase and the amplitude of the vibration was changing rapidly. Its track was nearly an ellipse and went around an almost fixed center. As the speed was increased, the ellipse orbit became bigger while the center of the ellipse was still there. When the rotor system entered the whirl region, the size of the ellipse orbit was almost fixed.

Fig. 11 shows the acceptance region plot combining the transient positions of the shaft centerlines while the rotor system was running from 2792 to 2962 rpm, which can be used as a control index and can be set here according to different running conditions. The phenomena were observed as follows: first, these dots (the transient positions of the shaft centerlines) were almost in the same positions and were nearly fixed in a small region. The rotor system to be observed was stable. Next, with the increasing rotor speed, the rotor system entered the transitional region. These dots fluctuated rapidly and were left outside the acceptance region. Finally, when the rotor system was in the whirl region, these dots moved in an ellipse track and were outside the acceptance region. Through this technique, the instability existing in the fluid-film bearing of the rotor system can easily be predicted and prevented.

There are many techniques to treat the problems of fluid-induced instability, such as an anti-swirl injection, externally pressurized bearing with anti-swirl, proper loading of hydrodynamic bearings, adjustment of supply pressure, change in the shape of bearing, and adjustment of lube oil temperature; some of them need the parameter as a control index to predict and control the bearings. The transient position of a shaft centerline combining an acceptance region is a very good choice.

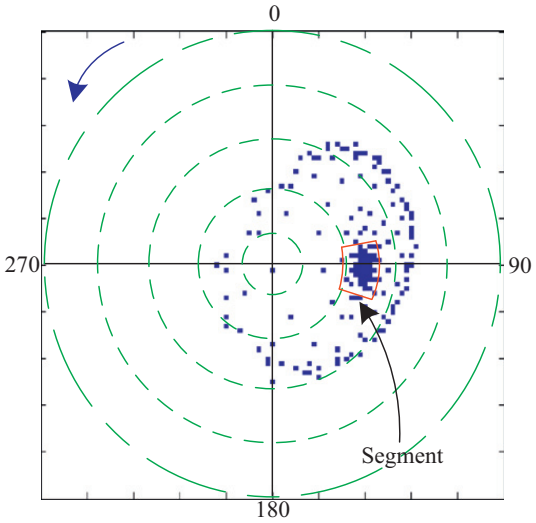

Fig. 11. An acceptance region plot with the transient positions of shaft centerlines.

5. Conclusion

In this paper, the phenomena in start-up vibration responses were investigated. The important results are summarized as follows. First, through this experiment, a variety of plots and the instability phenomena existing in rotating machinery are illustrated in detail. This enhances the ability of bearing designers to treat the fluid-induced instability problems. Next, the full Hilbert spectrum, which was developed in this study, definitely demonstrates the symptom of dry whip, which cannot be revealed on the Hilbert spectrum. Moreover, the transient position of a shaft centerline combining an acceptance region can clearly illustrate the transition, helps bearing designers know how fluid-induced instability occurs, and provides a new technique for predicting these kinds of problems. As a result, these findings can be applied to the design of controllable bearings. Thus, the life of rotating machinery can be extended and the instability problems existing in rotating machinery should no longer be vexing problems. In the future, the techniques presented in this paper to develop new control means of bearings can be explored.

References

[1] A. Muszynska, Whirl and whip—rotor/bearing stability problems, Journal of Sound and Vibration 110 (3) (1986) 443–462.
[2] A. Muszynska, Stability of whirl and whip in rotor/bearing systems, Journal of Sound and Vibration 127 (1) (1988) 49–64.
[3] N.E. Huang, A new view of nonlinear waves: the Hilbert spectrum, Annual Review of Fluid Mechanicals 31 (1993) 417–457.
[4] N.E. Huang, Z. Shen, The empirical mode decomposition and the Hilbert Spectrum for non linear non-stationary time series analysis, Proceedings of the Royal Society of London 454 (1998) (1971) 903–995.
[5] D.E. Bently, C.T. Hatch, Fundamentals of Rotary Machinery Diagnostics, Bently Pressurized Bearing Company, Minder, NV, 2002.
[6] H. Rylander, M. Carlson, C.R. Lin, Actively controlled bearing surface profiles theory and experiments, Tribology Symposium 72 (1995) 11–14.
[7] I.F. Santos, R. Nicoletti, Self-excited vibrations in active hydrodynamic bearings, Journal of the Brazilian Society of Mechanical Sciences 18 (3) (1996) 263–272.
[8] D.C. Deckler, R.J. Veillette, M.J. Braun, F.K. Choy, Simulation and control of an active tilting-pad journal bearing, Tribology Transactions 47 (3) (2004) 440–458.
[9] Z. Cai, M.S. De Queiroz, M.M. Khonsari, On the active stabilization of tilting-pad journal bearings, Journal of Sound and Vibration 273 (1-2) (2004) 421–428.
[10] D.E. Bently, C.T. Hatch, Shaft levitation made simple, Turbomachinery International 47 (5) (2006) 30–32.
[11] J.L. Lawen Jr, G.T. Flowers, Interaction dynamics between a flexible rotor and an auxiliary clearance bearing, Journal of Vibration and Acoustics 121 (2) (1999) 183–189.
[12] A. Muszynska, Rotor-to-stationary element rub-related vibration phenomena in rotary machinery, Shock and Vibration Digest 21 (3) (1989) 3–11.
[13] A. Lingener, Experimental investigation of reverse whirl of a flexible rotor, in: Proceedings of the IFToMM Third International Conference on Rotordynamics, Lyon, France, 1990, pp. 13–18.
[14] S. Crandall, From whirl to whip in rotordynamics, in: Proceedings of the IFToMM Third International Conference on Rotordynamics, Lyon, France, 1990, pp. 19–26.
[15] D. Childs, Turbomachinery Rotordynamics: Phenomena, Modeling, and Analysis, John Wiley and Sons, New York, 1993.
[16] J.J. Yu, P. Goldman, D.E. Bently, A. Muzynska, Rotor/seal experimental and analytical study on full annular rub, Journal of Engineering for Gas Turbines and Power 124 (2) (2002) 340–350.
[17] H.F. Black, Interaction of a whirling rotor with a vibration stator across a clearance annulus, Journal of Mechanical Engineering Science 10 (1968) 1–12.
[18] Y.S. Choi, Experimental investigation of partial rotor rub, KSME International Journal 14 (11) (2000) 1250–1256.
[19] Z.K. Peng, F.L. Chu, P.W. Tse, Detecting of the rubbing-caused impacts for rotor–stator fault diagnosis using reassigned scalogram, Mechanical Systems and Signal Processing 19 (2) (2005) 391–409.
[20] D. Yu, J. Cheng, Y. Yang, Application of EMD method and Hilbert spectrum to the fault diagnosis of roller bearing, Mechanical Systems and Signal Processing 19 (2) (2005) 259–270.
[21] G. Gai, The processing of rotor startup signals based on empirical mode decomposition, Mechanical Systems and Signal Processing 20 (1) (2006) 222–235.

[22] K. Qi, Z. He, Y. Zi, Cosine window-based boundary processing method for EMD and its application in rubbing fault diagnosis, Mechanical Systems and Signal Processing 21 (7) (2007) 2750–2760.
[23] T.H. Patel, A.K. Darpe, Study of coast-up vibration response for rub detection, Mechanism and Machine Theory 44 (8) (2009) 1570–1579.
[24] D.E. Bently, Shaft crack detection using the acceptance region, Orbit (1987).
[25] P. Goldman, A. Muszynska, Application of full spectrum to rotating machinery diagnostics, Orbit, First Quarter (1999).
[26] J. Tuma, J. Bilos, Full Spectrum Analysis in Journal Bearing Diagnostics, ICCC, 2004.